Using 3D Models to Analyse Stratigraphic and Sedimentological Contexts in Archaeo-Palaeo-Anthropological Pleistocene Sites (Gran Dolina Site, Sierra De Atapuerca)

I. Campaña[(1)]

A. Benito-Calvo[(1)]

A. Pérez-González[(1)]

A. I. Ortega[(1)]

J.M. Bermúdez de Castro[(1)]

E. Carbonell[(2,3)]

[1] Centro Nacional de Investigación sobre la Evolución Humana (CENIEH), Burgos, España.
[2] IPHES, Institut Català de Paleoecología Humana i Evolució Social, Tarragona. España.
[3] Universitat Rovira i Virgili (URV), Campus Catalunya, Tarragona, España.

Abstract: Gran Dolina is a cavity that belongs to the second level of the Sierra de Atapuerca multi-level karst system and shows an Early and Middle Pleistocene sedimentary infilling 25 m thick, divided in eleven lithostratigraphic units. High densities of remains have been found in Gran Dolina, including hominid bones, fauna and lithic tools.

The use of 3D models in stratigraphy and sedimentology is a new topic that allows new analysis and studies, increasing the knowledge of archaeological sites. In Gran Dolina site, the application of 3D laser scanning and photogrammetry techniques have allowed performing 3D models, including RGB textures. The models were georeferenced to the excavation local coordinate system. From these 3D models, we identified and mapped the continuity and geometry of the sedimentary levels, reconstructing the site's original stratigraphy. The 3D geometry of the levels was used to measure the clasts' textures and the post-depositional dips of the layers. The latter helped us to infer input strikes as well as their variations in each level, and to recognize ancient sedimentary entrances.

Keywords: Laser scanner, Photogrammetry, Stratigraphic geometries, Gran Dolina site, Atapuerca, Early and Middle Pleistocene.

Introduction

Gran Dolina is a key site to understand Early and Middle Pleistocene human evolution in Europe (Rodríguez *et al*. 2011). The archaeo-paleontological remains of Gran Dolina have provided many works about Early and Middle Pleistocene that have enriched the knowledge about human linage in Europe (Bermúdez de Castro *et al*. 2012; Bermúdez de Castro *et al*. 2015; Carbonell *et al*. 1999; Rodríguez-Gómez *et al*. 2013). Gran Dolina is a cavity belonging to the intermediate level of the Sierra de Atapuerca multi-level karst system (Ortega *et al*. 2013), which shows an Early and Middle Pleistocene 25 m thick sedimentary infilling, divided in eleven lithostratigraphic units and nineteen sedimentary facies (Pérez-González *et al*. 2001; Campaña *et al*. 2015). Although most of these units are archaeologically fertile and have provided a huge number of fossils and stone tools, TD6 and TD10 units are renowned for its richness and importance. A new hominid was defined, *Homo antecessor* (Carbonell *et al*. 1995; Bermúdez de Castro *et al*. 1997), with the remains found in TD6, while TD10 has provided two high density layers of archaeological and palaeontological remains (Ollé *et al.* 2013), related to the presence of *Homo heidelbergensis*.

The Sierra de Atapuerca is situated in Burgos (Spain), at the north of the Iberian Peninsula. It consists of a carbonated Mesozoic inlier represented by a gentle anticlinal ridge (Fig. 1, Benito-Calvo and Pérez-González 2015), that belongs to the most north-western outcrop of the Iberian Chain. It is situated in the NE Neogene Duero Basin. Here, a multi-level endokarst system is formed, composed by three sub-horizontal levels and 4.7 km of explored passages (Martín-Merino *et al*. 1981; Ortega *et al*. 2013). The opening of the caves to the outside during the Early Pleistocene due to regional fluvial incision and slope retreatment (Benito-Calvo *et al*. 2015), resulted in allochthonous sediment inputs and the accumulation of archaeo-paleoanthropological remains. Finally, a railway trench built during 19th century cut the intermediate level and exposed several karstic infills such as the ones related to Gran Dolina, Galeria Complex and Sima del Elefante sites.

The use of 3D models in stratigraphy and sedimentology is a new topic that allows new analysis and studies, increasing the knowledge of archaeological sites (Westoby *et al.* 2012; Pavelka *et al.* 2014; Neubauer 2007). In this work we analyse the geometry and texture of the stratigraphic layers using 3D models and orthophotos acquired by photogrammetry.

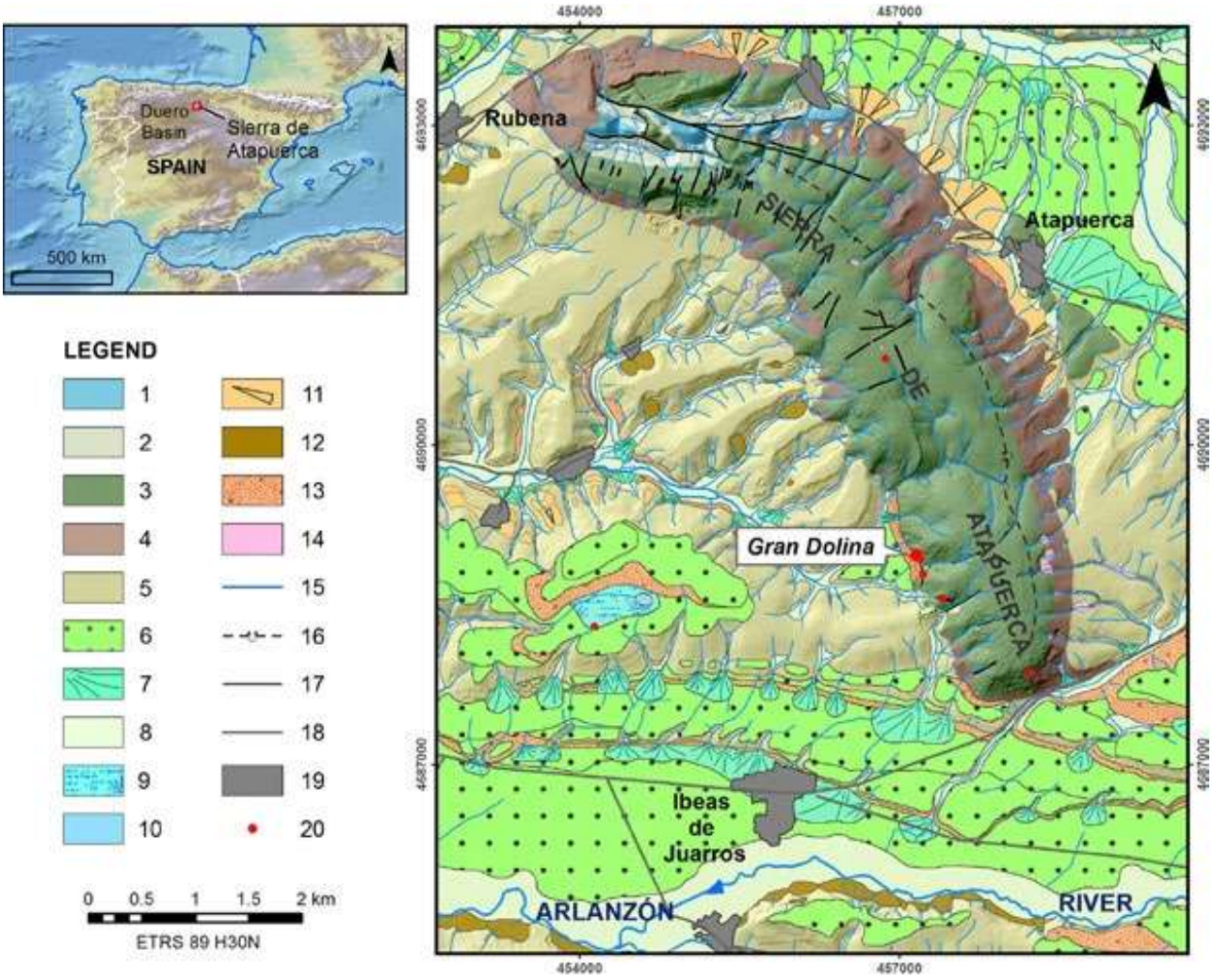

FIG. 1. GENERAL LOCATION AND GEOLOGICAL MAP OF THE SIERRA DE ATAPUERCA (SIMPLIFIED FROM BENITO-CALVO AND PÉREZ-GONZÁLEZ 2015). LEGEND: 1, JURASSIC; 2, EARLY CRETACEOUS; 3, LATE CRETACEOUS; 4, OLIGOCENE; 5, MIOCENE; 6, FLUVIAL TERRACES; 7, CONES; 8, FLOODPLAINS AND VALLEY FLOORS; 9, SEMI-ENDORHEIC AREAS; 10, SEASONAL POOLS; 11, GLACIS; 12, LANDSLIDES; 13, COLLUVIUM; 14, DOLINA FLOORS; 15, DRAINAGE NETWORK; 16, INFERRED OVERTURNED ANTICLINE; 17, FAULTS; 18, ROADS, 19, POPULATIONS; 20, ARCHAEOLOGICAL SITES.

1 Methodology

3D models of Gran Dolina site were performed using photogrammetry and laser scanner technologies. The three excavation surfaces (TD1, TD4 and TD10) were photographed with a Nikon D3X camera at different distances and angles. Then, the images were selected to avoid recurrent data and wrong images, and they were processed by Agisoft Photoscan 1.0.4 software. 3D models were improved and georeferenced using control points extracted from scanner cloud points.

We used two different laser scanners, Leica Scanstation C10 and Faro Focus X330, in the three surfaces. Leica Scanstation C10 is a time-of-flight laser scanner which point clouds are processed by the Cyclone 7.4 software. Faro Focus X330 is phase-shift scanner that uses Scene 5.4.2 software in its post-process. For both laser scanners, cloud points were acquired from different places in each surface and middle resolution configuration (~1 cm at 10 m) was used. Later, cloud points were cleaned and registered. The archaeological local coordinate system was introduced by targets.

Stratigraphic sections and measurements were carried out in ArcGIS 10.2, using orthophotos previously processed in Agisoft Photoscan. Sedimentary facies have been defined in previous work (Campaña *et al*. 2015).

2 Results and discussion

The use of laser scanners and photogrammetry technologies allowed us to perform measurements and analyses that would other way be very difficult or tedious achieve (Larsson *et al.* 2015; Bennett *et al.* 2013). Post-depositional dips, strikes, and clast textures were measured in the 3D models and orthophotos in order to estimate sedimentary input strikes.

2.1 3D models

Three 3D models were performed using photogrammetric techniques (Fig. 2, 3 and 4).

The use of laser scanners has allowed comparing the accuracy of the models. TD1 and TD4 photogrammetric models have an

Fig. 2. TD1 model by photogrammetry. 41 images used.

Fig. 4. TD10 model by photogrammetry. 39 images used.

Fig. 3. TD7-TD4 model by photogrammetry. 44 images used.

excellent fit, but TD10 model shows some difficulties. First, the boundary of the model shows an imprecise definition. Second, photogrammetry in the excavation area does not provide a realistic RGB texture. The first task could be corrected including more photos of the boundaries. The second difficulty was due to the irregular surface of TD10 in the excavation area, which is not present in the vertical sections of TD10 model. Anyway, the sections of TD10 are accurate and allow measurements.

2.2 Orthophotos

The stratigraphy and sedimentology of the Gran Dolina site were done using field observations and orthophotos. The dips of the units were calculated using the orthophotos in GIS software (Fig. 5, 6 and 7). For more details about the stratigraphy and sedimentary facies we refer to Campaña *et al*. 2015.

The dips of the layers in TD10 are similar in the east and the south section, indicating that the sediment input strike is towards the corner (see below). Post-depositional deformation is not found.

The TD7 to TD4 section shows a change of sin-depositional dip beside others post-depositional dips. TD5 and the lower layers of TD6 have a dip of 10°N. These layers are mainly grain-supported gravels with clayed silts and matrix-supported boulders. Gravels with lateral silts are interpreted as channel flow and floodplain facies (Campaña *et al*. 2015), which had surely a horizontal deposition. Therefore the actual dip of 10°N of this facies could be explained by post-depositional accommodation of the sediments. The TD5 deformation occurs in the north of the section and migrates progressively towards the south in TD6 layers.

TD6.2 and TD7 have other post-depositional dips (Fig. 6) and their origin is surely different to the previous layers. The south section is composed by mud and silt layers. These layers are more compacted than the ones with more limestone clasts. Their compaction could have caused the post-depositional deformation of TD6.2 and TD7.

TD1 sediments are fluvial laminated sands and silts, which are tilted and deformed toward the center of the cavity. Considering these characteristics and a putative horizontal deposition of these facies, the current tilting observed in these layers, could be explained as post-depositional processes. The dips decrease in the upper layers, which suggests sin-depositional deformation caused by the accommodation of the sediments and the silting. Moreover, the dips increase towards the west, where the centre of cavity is found, indicates more accommodation or elimination of the sediment towards the centre of the cavity and post-depositional folds.

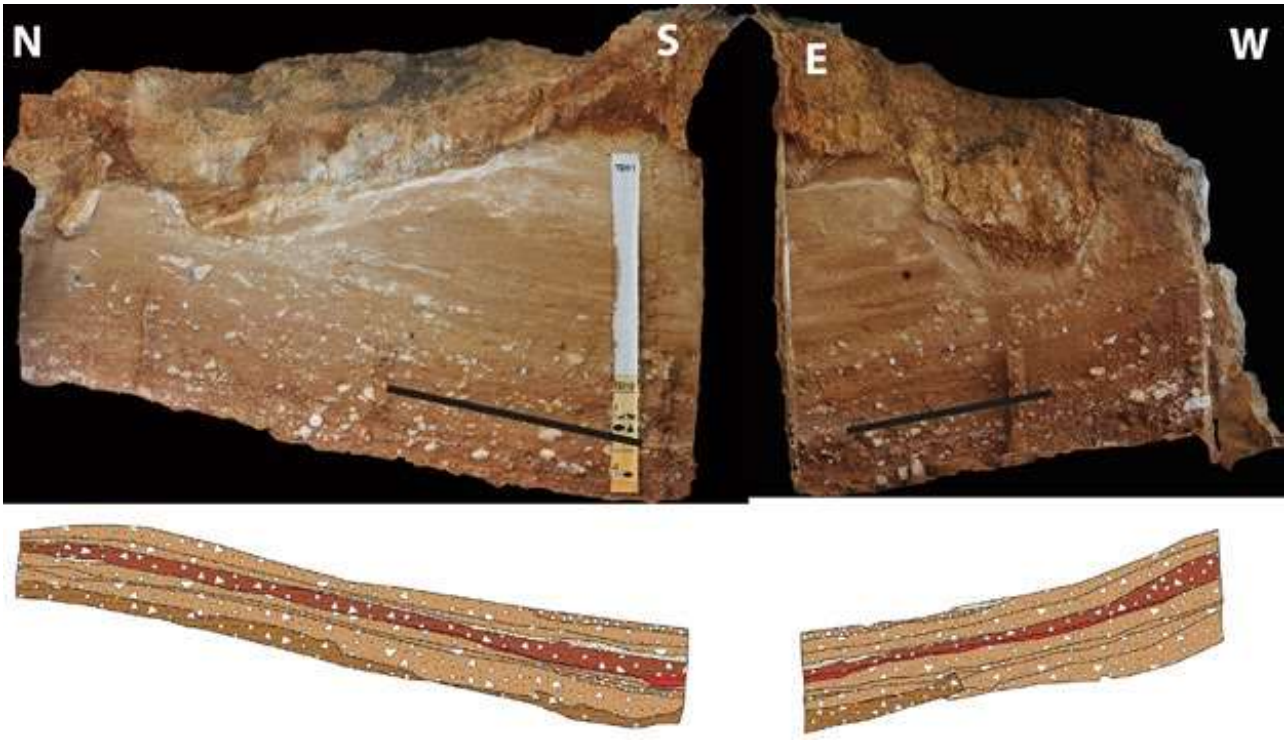

Fig. 5. East and south section of TD10. East section dip: 11° S. South section dip: 11° E.

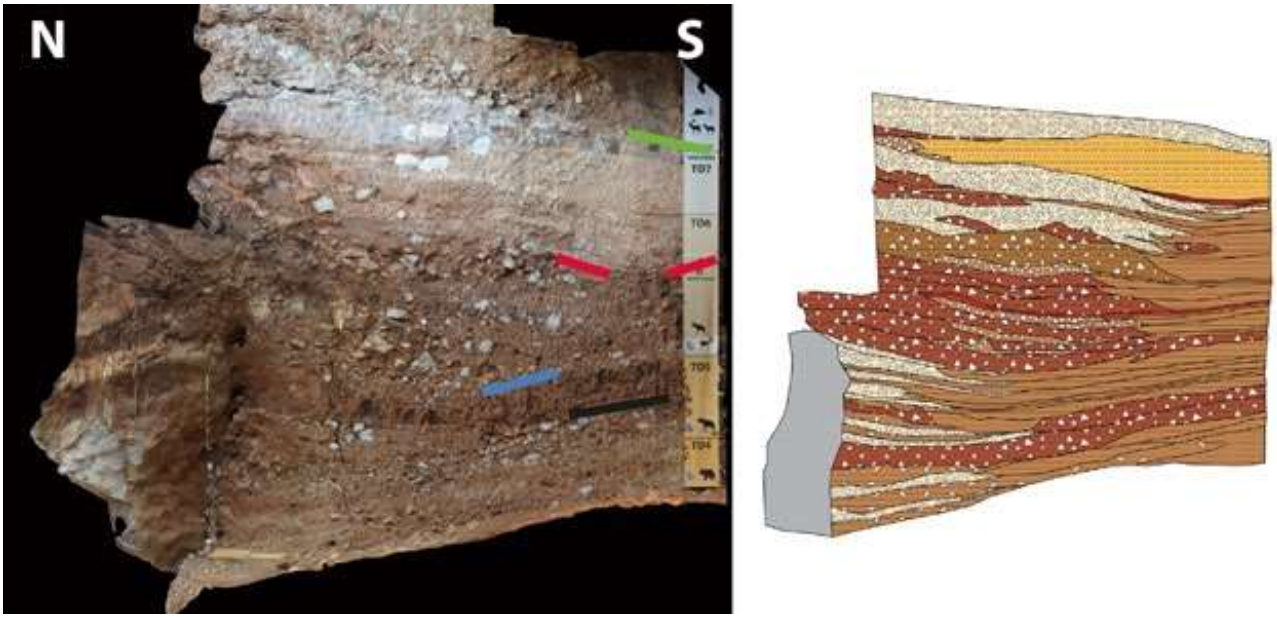

Fig. 6. TD7 to TD4 section. Silty layers have post-depositional deformation. TD7 dip: 11° S. TD6.2 dip: 15°. N-S TD6 base dip: 10°. N TD5 dip: 10° N.

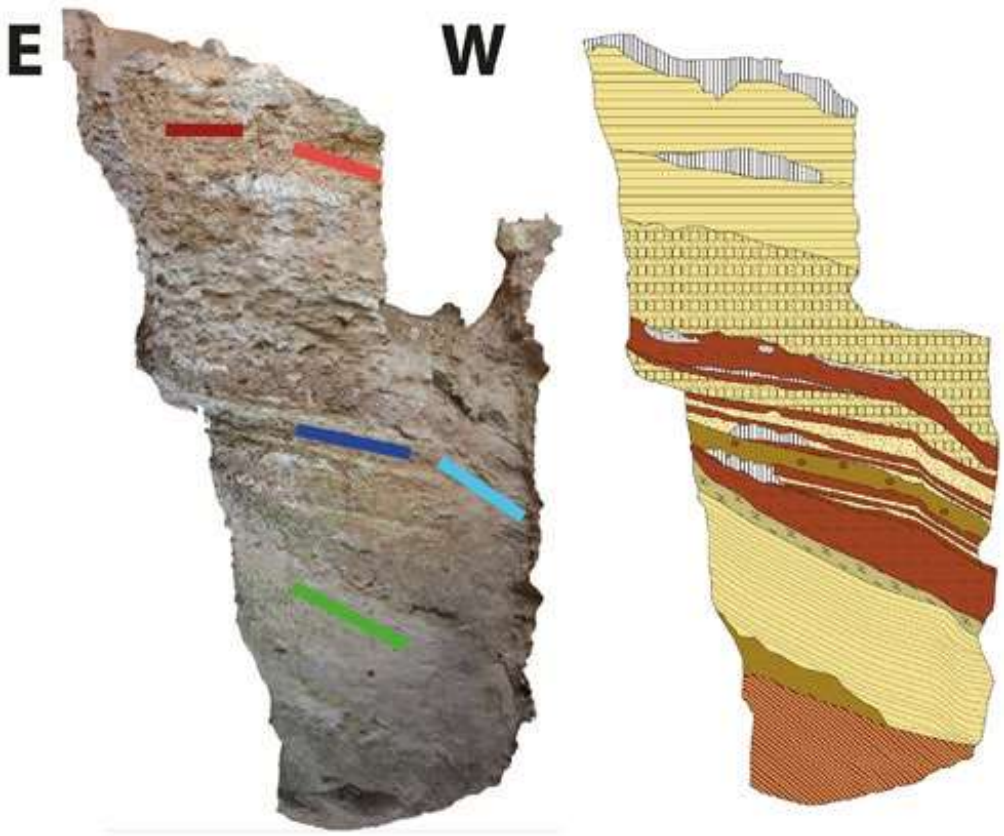

Fig. 7. TD1 section. Lower layers have a dip of 30° W. Middle layers have a dip of 12° W, and to the west increased to 33° W. Upper layers have a dip of 0°, and to the west increased to 15° W.

2.3 Clast texture

Campaña *et al*. (2015) defined six debris flow sedimentary facies in Gran Dolina site, where the clast percentage for each facies is estimated by field observations. The combined use of orthophotos and GIS software has allowed us to quantify the clast percentage of the sections (Table 1). In this work, the clast percentage of the four debris flow sedimentary facies (B, C, D and F) was calculated (Fig. 8, 9 and 10).

Tab. 1. Clast percentage for each debris flow facies analysed.

	%Clast
Debris flow Facies B	10-20
Debris flow Facies C	35-45
Debris flow Facies D	20-30
Debris flow Facies F	10-30

The results support the debris flow facies classification showing similar values to the field observation (Table 1) (Campaña *et al*. 2015). Variations in the clasts percentage could be due to changes in the sediment source, energy flow or cave entrance. High percentage of clasts, as debris flow facies C, suggests a high energy flow that dragged all the available sediments through a large entry. Low percentage of clasts, as debris flow facies B, indicates more fine sediment in the source, lower energy flow and therefore, there was no need of a large entry.

2.4 Sediment input strike

Sediment input strikes were mathematically calculated using the apparent dips and the strikes of both TD10 sections (Tab. 2). The dips were measured in the orthophotos using the layer geometries observed in the two sections. The resulted sediment input strikes have been projected in the 3D model.

Tab. 2. Strikes and dips calculated using TD10 sections.

Layer	Strike	Dip (E)
TD10-TD11	N45°E	12°
TD10.1.2	N39°E	15°
TD10.1.3	N39°E	14°
TD10.1.4	N40°E	15°
TD10.1.6	N38°E	16°
TD10.1 'Manta 1'	N33°E	15°
TD10.2.2	N35°E	18°
TD10.2.5	N45°E	20°

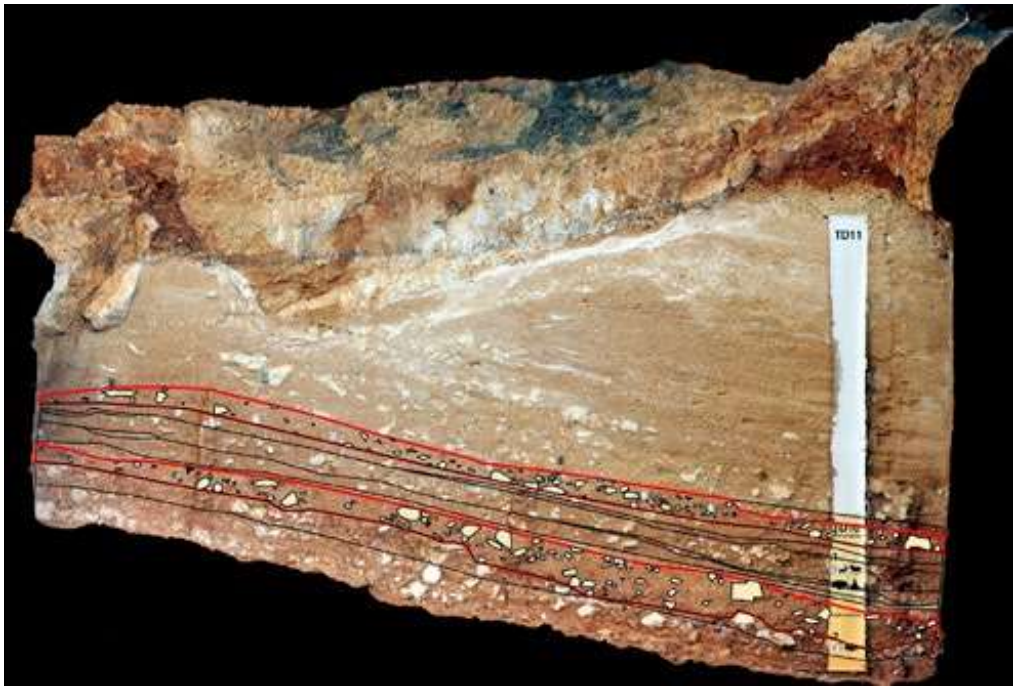

Fig. 8. NE section of TD10 with the stratigraphic limits. Red lines indicate the layers where clast texture was measured. The identified clasts are marked.

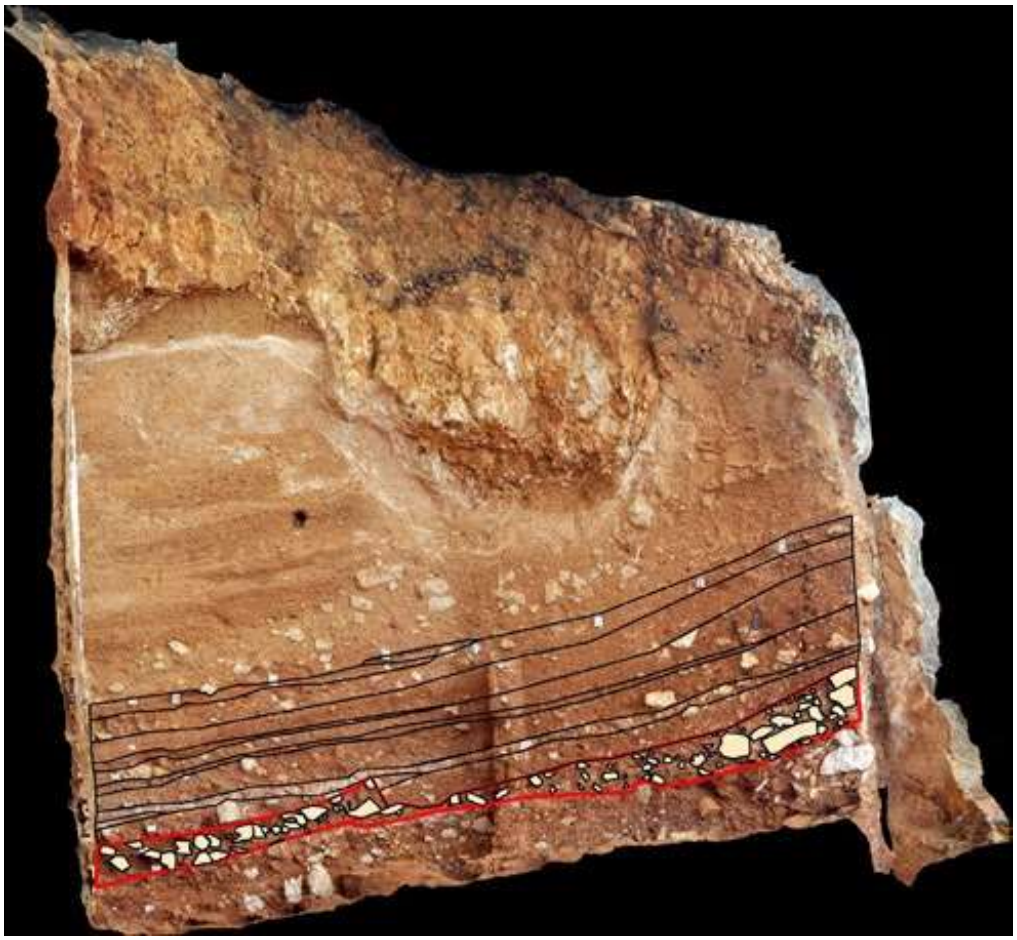

Fig. 9. SE section of TD10 with the stratigraphic limits. Red lines indicate the layers where clast texture was measured. The identified clasts are marked.

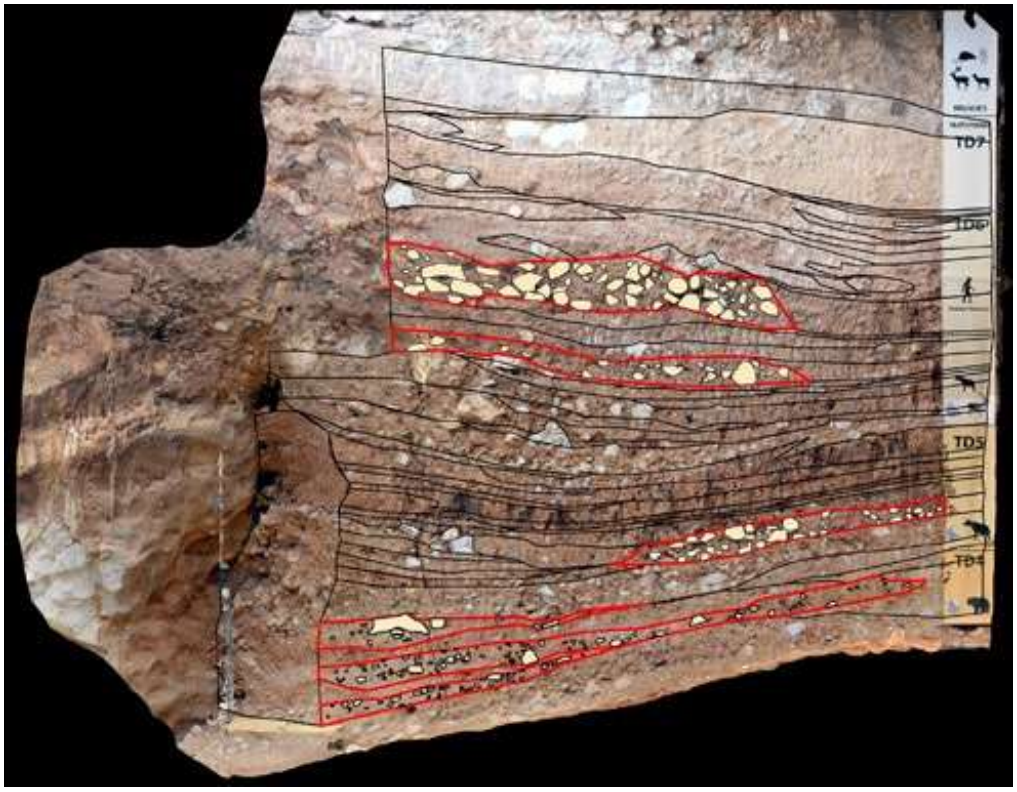

Fig. 10. TD7-TD4 section with the stratigraphic limits. Red lines indicate the layers where clast texture was measured. The identified clasts are marked.

The strike ranges from 33° to 45° with respect to the Y axis, while the dip values are situated between 12-20° towards the East. Not trend is observed in the strike (Fig. 11), providing a range between N45°E and N33°E which indicates the entry of the sedimentary inputs. Small variations may have been caused by the accommodation to the local paleo-relief. Besides, the debris flow clast percentage previously calculated suggests a large entry, which would have enabled the access and settlement of hominids in the cave (Ollé *et al*. 2013).

TD10 dips show differences, varying from 20º from TD10.2, to 15° for TD10.1. A decrease of the dip towards the upper layers is observed (Fig. 11). This can be related with the progressive filling of the cave and its main entry, which could explain the progressive decrease of the use of the cavity by the Middle Pleistocene hominins (Ollé *et al*. 2013). During the human occupation, the palaeo-relief was a gentle slope towards the east, with an irregular surface of disorganized clasts.

3 Conclusions

The application of 3D laser scanning and photogrammetry techniques have allowed us to carry out 3D models, including RGB textures. From these 3D models, we have identified and mapped the continuity and geometry of the sedimentary levels, reconstructing the stratigraphy of Gran Dolina.

Particle size analysis of large clasts cannot be analysed by laboratory methods, because a large size and the amount of sample would be needed. Orthophotos and GIS software allow an approximation to quantify clast percentage in the sedimentary units. The clast percentage supports the classification of sedimentary facies proposed in Campaña *et al.* (2015) and allow inferring the energy flow and entrance.

TD1 has a sin-depositional deformation and at least two post-depositional deformations. The sin-depositional deformation is indicated by the progressive decrease of the deformation dip towards the upper layers and is related to accommodation and filling. Post-depositional deformations are represented by two different dips in the middle layers. These deformations could be due to a loss of sediment volume in the centre of the conduct of Gran Dolina, either by accommodation or elimination of the sediments.

In TD7 to TD4 section, the dips indicated that two main post-depositional deformation processes have happened. First, processes affected TD5 and the base of TD6, inclining 10 grades the layers. Second, processes affected TD6.2, TD6.1 and TD7. Both folds could be explained by the accommodation of the finer deposits (silt and clay layers) and the first deformation is surely produced before the TD6.3.1 inputs. This could indicate a stable period without sediments inputs. The increase of clasts percentage in this section (facies B, D and C) suggests that an increase of the energy flow and size of the entry occurred during the final of Early Pleistocene. This enlargement of the entry could make the human presence in TD6.2 and TD6.1 possible.

TD10 sediment input strikes have been obtained using 3D stratigraphic boundaries of both sections. The strikes are very similar between them, indicating that the main entrance was

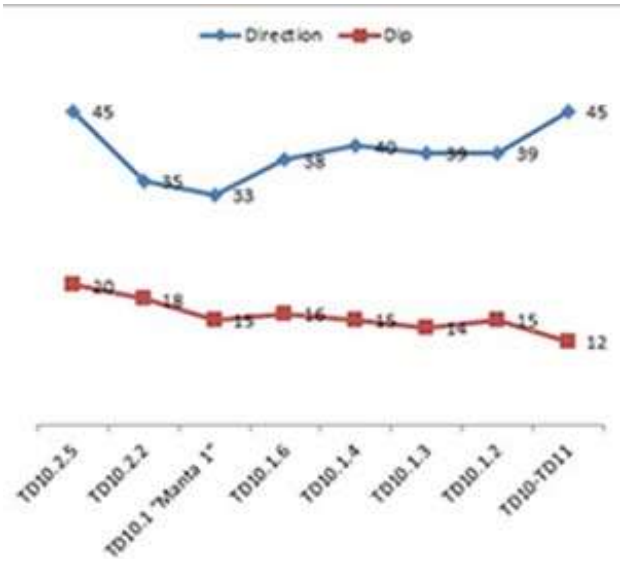

FIG. 11. DIPS AND DIRECTIONS OF THE SEDIMENT INPUTS OF TD10 LAYERS.

the same during this period. The little variations could be due to the accommodation of the sediment input to the paleo-relief. The dips show a decrease from TD10.2 to the boundary of TD10-TD11 (Fig. 11, Tab. 2) that was caused by the silting up of the west entrance. This progressive narrowing of the entrance could be related to the decrease of human presence in Gran Dolina.

Acknowledgements

This study was supported by the MINECO project, CGL2012-38434-C03-02. I. Campaña is the beneficiary of a predoctoral FPI Grant from the Spanish MINECO. Fieldwork at Atapuerca is supported by the Consejería de Cultura y Turismo of the Junta de Castilla y León. 3D models and spatial analysis were carried out using the facilities of the Laboratory of Digital Mapping and 3D Analysis (CENIEH). This work has benefited from discussion with Lucía Bermejo Albarrán and two anonymous reviewers.

Bibliography

Bennett, M. R., P. Falkingham, S. A. Morse, K. Bates, Crompton. R.H. 2013. Preserving the Impossible: Conservation of Soft-Sediment Hominin Footprint Sites and Strategies for Three-Dimensional Digital Data Capture. PLoS (Public Library of Science) ONE 8, 4: e60755.

Bermúdez de Castro, J. M., Arsuaga, J. L., Carbonell, E., Rosas, A., Martínez, I., Mosquera, M. 1997. A Hominid from the Lower Pleistocene of Atapuerca, Spain: Possible Ancestor to Neandertals and Modern Humans. *Science* 276 (5317): 1392–5.

Bermúdez de Castro, J. M., Carretero, J. M., García-González, R., Rodríguez-García, L., Martinón-Torres, M., Rosell, J., Blasco, R., Martín-Francés, L., Modesto, M., Carbonell, E. 2012. Early Pleistocene Human Humeri from the Gran Dolina-TD6 Site (sierra de Atapuerca, Spain). *American Journal of Physical Anthropology* 147 (4): 604-17.

Bermúdez de Castro, J. M., Martinón-Torres, M., Martín-Francés, L., Modesto-Mata, M. Martínez-de-Pinillos, M., García, C., Carbonell, E. 2015. Homo Antecessor: The State of the Art Eighteen Years Later.' *Quaternary International* 0. doi:10.1016/j.quaint.2015.03.049.

Benito-Calvo, A., Pérez-González, A., 2015. Geomorphology of the Sierra de Atapuerca and the Middle Arlanzón Valley (Burgos, Spain). *Journal of Maps* 11: 535–44. doi:10.1080 /17445647.2014.909339.

Benito-Calvo, A., Ortega, A.I., Pérez-González, A., Campaña, I., Bermúdez De Castro, J.M., Carbonell, E., 2015. Palaeogeographical reconstruction of the Pleistocene sites in the Sierra the Atapuerca (Burgos, Spain). *Quaternary international*. In press.

Campaña, I., Benito-Calvo, A. Pérez-González, A., Ortega, A. I., Bermúdez de Castro, J. M., Carbonell, E. 2015. Pleistocene Sedimentary Facies of the Gran Dolina Archaeo-Paleoanthropological Site (Sierra de Atapuerca, Burgos, Spain). *Quaternary International.* In press.

Carbonell, E., Bermúdez De Castro, J. M., Arsuaga, J. L., Diez, J. C., Rosas, A., Cuenca-Bescós, G., Sala, R., Mosquera, M., Rodríguez, X. P. 1995. Lower Pleistocene Hominids and Artifacts from Atapuerca-TD6 (Spain). *Science* 269 (5225): 826–30.

Carbonell, E., García-Antón, M. D., Mallol, C., Mosquera, M., Ollé, A., Rodríguez, X. P., Sahnouni, M., Sala, R., Vergès, J. M. 1999. The TD6 Level Lithic Industry from Gran Dolina, Atapuerca (Burgos, Spain): Production and Use. *Journal of Human Evolution* 37 (3-4): 653–93.

Larsson, L., Trinks, I., Söderberg, B., Gabler, M., Dell'Unto, N., Neubauer, W., Ahlström, T. 2015. Interdisciplinary Archaeological Prospection, Excavation and 3D Documentation Exemplified through the Investigation of a Burial at the Iron Age Settlement Site of Uppåkra in Sweden. *Archaeological Prospection 22(3)*: 143-56.

Martín-Merino, M. A., Domingo, S., Antón, T. 1981. Estudio de Las Cavidades de La Zona BU-IV A (Sierra de Atapuerca). *Kaite* 2: 41–76.

Neubauer, W. 2007. 'Laser Scanning and Archaeology: Standard Tool for 3D Documentation of Excavations.' *GIM International* 21 (10): 14–7.

Ollé, A., Mosquera, M., Rodríguez, X.P., de Lombera-Hermida, A., García-Antón, M. D., García-Medrano, P., Peña, L. 2013. The Early and Middle Pleistocene Technological Record from Sierra de Atapuerca (Burgos, Spain). *Quaternary International* 295: 138–67.

Ortega, A. I., A. Benito-Calvo, A. Pérez-González, M. A. Martín Merino, R. Pérez-Martínez, J. M. Parés, A. Aramburu, J. L. Arsuaga, J. M. Bermúdez de Castro, and E. Carbonell. 2013. 'Evolution of Multilevel Caves in the Sierra de Atapuerca (Burgos, Spain) and Its Relation to Human Occupation.' *Geomorphology* 196: 122–33. doi:10.1016/j.geomorph.2012.05.031.

Pavelka, K., Reznicek, J., Matouskova, E., Faltynova, M. 2014. Using of Close Range Photogrammetry in Image Based Modelling Form for Archaeology. In *35th Asian Conference on Remote Sensing 2014, ACRS 2014: Sensing for Reintegration of Societies*: 1353-8.

Pérez-González, A., Parés, J. M., Carbonell, E., Aleixandre, T., Ortega, A. I., Benito, A., Martin Merino, M. A. 2001. Géologie de La Sierra de Atapuerca et Stratigraphie Des Remplissages Karstiques de Galeria et Dolina (Burgos, Espagne). *L'Anthropologie* 105 (1): 27–43.

Rodríguez-Gómez, G., Rodríguez, J., Martín-González, J. T., Goikoetxea, I., Mateos, A. 2013. Modeling Trophic Resource Availability for the First Human Settlers of Europe: The Case of Atapuerca TD6. *Journal of Human Evolution* 64 (6): 645–57. doi:10.1016/j.jhevol.2013.02.007.

Rodríguez, J., Burjachs, F., Cuenca-Bescós, G., García, M., Van der Made, J., Pérez González, A., Blain, H. A., Expósito, I., López-García, J. M., García Antón, M., Allué, E., Cáceres, I., Huguet, R., Mosquera, M., Ollé, A., Rosell, J., Parés, J. M., Rodríguez, X. P., Díez, C., Rofes, J., Sala, R., Saladié, P., Vallverdú, J., Bennasar, M. L., Blasco, R., Bermúdez de Castro, J. M., Carbonell, E. 2011. One Million Years of Cultural Evolution in a Stable Environment at Atapuerca (Burgos, Spain). *Quaternary Science Reviews* 30 (11-12): 1396-1412.

Westoby, M. J., Brasington, J., Glasser, N. F., Hambrey, M. J., Reynolds, J.M. 2012. 'Structure-from-Motion' Photogrammetry: A Low-Cost, Effective Tool for Geoscience Applications. *Geomorphology* 179 (0): 300–14.